The scaling of embedded collisionless reconnection

M. A. Shay,[a] J. F. Drake, and M. Swisdak
Institute for Research in Electronics and Applied Physics, University of Maryland, College Park, Maryland 20742

B. N. Rogers
Department of Physics and Astronomy, Dartmouth College, Hanover, New Hampshire 03755

(Received 25 November 2003; accepted 20 February 2004; published online 16 April 2004)

The scaling of the reconnection rate is examined in situations in which the equilibrium current supporting a reversed magnetic field has a spatial scale length that is much greater than all nonmagnetohydrodynamic (non-MHD) kinetic scales. In this case, denoted as embedded reconnection, the narrow non-MHD region around the x-line where dissipation is important is embedded inside of a much larger equilibrium current sheet. In this system, the magnetic field just upstream of this non-MHD region, B_d, changes significantly during the reconnection process. This wide equilibrium current sheet is contrasted with the very thin equilibrium current sheets of width c/ω_{pi} used in previous simulations to establish the importance of the Hall term in Ohm's law in allowing fast reconnection in large scale collisionless systems. In the present study we lay out a procedure for determining B_d directly from simulation data and use this value to renormalize the reconnection rate using Sweet–Parker-like scaling arguments. Using two-dimensional two-fluid simulations, we find that the time evolution of the reconnection process can be broken into two phases: A developmental phase that is quite long and strongly dependent on system size and presumably the dissipation mechanisms, and a fast asymptotic phase in which the flow velocity into the x-line is on the order of 0.1 of the Alfvén speed based on B_d. The reconnection rate during the asymptotic phase is independent of system size and the majority of island growth and flux reconnection occurs during this phase. The time to reconnect a significant amount of magnetic flux is roughly consistent with solar flare timescales. © *2004 American Institute of Physics.*
[DOI: 10.1063/1.1705650]

I. INTRODUCTION

Magnetic reconnection is a ubiquitous process in which magnetic field lines embedded in a plasma break and reform, releasing large amounts of energy in the form of plasma flows and particle heating. During reconnection, a nonmagnetohydrodynamic (non-MHD) region called the ion dissipation region forms near the x-line with a length of D along the outflow direction and a width of δ along the inflow direction. The geometry of this region is very important for determining the scaling of the rate of reconnection. A Sweet–Parker-like analysis of the flow into and out of this dissipation region yields[1] $V_{\mathrm{in}} \sim (\delta/D) c_{\mathrm{Ad}}$, where $c_{\mathrm{Ad}} = B_d/\sqrt{4\pi m_i n}$ and B_d is the magnetic field at the upstream edge of the ion dissipation region. We will review this derivation in Sec. III. Sweet–Parker-like analyses have been used extensively to understand the reconnection process.[2–6]

Many energy release events in nature that are believed to be produced through reconnection exhibit two disparate timescales: A very long period during which magnetic energy builds up but very little energy is released; and a sudden period of significant energy release. The key point is that most of the magnetic energy is released in this latter stage. Examining the build-up and energy release phases in the context of two space plasma systems yields interesting insights. In typical X-class solar flares, a large energy release in the form of x-rays and electron energization occurs for a period of about 100 seconds,[7] but an active region on the sun may exist for weeks without producing such a flare. During a magnetospheric substorm, a significant fraction of lobe flux is reconnected in a period of about 10 minutes causing a massive dipolarization of the magnetotail and significant energetic particles that create the aurora, but the typical time between repeating substorms is about 3 hours.[8]

In the context of this paper, we do not explicitly compress the current sheet to build up magnetic energy. Nevertheless, we also find that reconnection displays two distinct phases: A long developmental phase in which a finite magnetic island slowly forms and flows develop and a fast reconnection phase where most of the energy is released. Because of the small size of the island and very weak flows during the developmental phase, in any real system this phase will not be distinguishable from the build-up phase.

Gaining a physical understanding of the nature of the build-up and developmental phases is a very difficult but rich problem. The theory must predict rates fast enough to allow reconnection to grow from noise to significant size during the developmental phase, but it also must be slow enough to allow significant magnetic loading during the build-up phase between energy release events. Obtaining a theory that satis-

[a]Electronic address: shay@glue.umd.edu; URL: http://www.glue.umd.edu/~shay

fies these timescale demands is difficult, because the developmental phase is strongly dependent on the specific initial conditions and parameters in the system, and these conditions are to a large extent unknown, e.g., the size of the perturbations or forcing creating the x-line,[9] the thickness of the initial current sheet,[10] the size of the system,[11] the presence of a magnetic field normal to the current sheet,[12,13] and the specific kinetic equilibrium of the electrons.[14] The growth of reconnection from noise has also been shown to be strongly dependent on the electron to ion mass ratio[15] and the resistivity.[16] Note that the literature on the developmental phase of reconnection is extensive, and the citations above are only included to give examples. Contrary to the developmental phase, the fast phase of reconnection is much simpler, and we seek primarily to address that problem in this paper, although we do have some discussion of the developmental phase in our simulations.

A fundamental question about the fast reconnection phase is: Can reconnection be fast enough to explain the energy release timescales seen in physical systems? In the case of solar flares and substorms this question reduces to: Is it possible for a significant fraction of the available magnetic flux to reconnect in 100 seconds and 10 minutes, respectively? In the context of this question, it is unimportant how long it takes the reconnection to initiate. Previous work focused explicitly on the fast phase was limited to systems with no guide field and with very narrow (of order c/ω_{pi} with ω_{pi} the plasma frequency) equilibrium current sheets with constant magnetic field upstream of the current sheet, i.e., B_d was constant for much of the reconnection process. These systems exhibited a long period of quasi-steady reconnection, where the reconnection rate and the physical configuration of the ion dissipation region were unchanging, making the study of the scaling of this asymptotic reconnection rate very straightforward. Specifically, B_d did not need to be determined because it was constant in time and between simulations. It was found that the Hall term facilitated fast quasi-steady reconnection, corresponding to an inflow velocity around $0.1c_A$, independent of L/d_i,[17] and the electron to ion mass ratio m_e/m_i,[18–22] where $d_\alpha = c/\omega_{p\alpha}$ and L is the system size. In other words, the asymptotic reconnection rate was independent of the mechanism breaking the frozen-in constraint and the system size. Note that in all of these systems the initial x-line perturbation that initiates reconnection had a wavelength of the system size. In addition, the particular simulation code used, whether full particle, hybrid, or two-fluid, did not change the gross reconnection rate as long as it included the Hall term.[20,23,24] Because this *asymptotic* reconnection rate was independent of everything but c_A, it was termed a "universal constant."[17] The physics of dispersive waves generated through the non-MHD Hall term in Ohm's law was shown to be the key effect allowing the reconnection rate to scale independently of system size and the dissipation mechanism.[17,23,25]

Reconnection rates on the order of $0.1c_A$ yield timescales for global energy release and magnetic reconfiguration that are consistent with those seen in many physical systems when the equilibrium current sheets are narrow compared to system size scales, i.e., the fast reconnection phase exhibits a nearly steady reconnection rate because B_d remains nearly constant in time. In a typical X-class flare, reconnection may drive a global energy release, in the form of hard and soft x-ray emissions that last around 100 seconds. With rough estimates of the magnetic field and density in the solar corona ($B \approx 100$ G and $n \approx 10^{10}$ cm^{-3}), the reconnection inflow velocity comes to around $2 \cdot 10^7$ cm/s. A typical magnetic flux tube involved in a flare has an area of 10^{18} cm^2 and a length of 10^9 cm, giving a time of 50 seconds to reconnect much of the magnetic field in the flux tube. This length of time is consistent with the duration of typical flares.[7] During a substorm, a significant fraction of lobe flux is reconnected causing a massive dipolarization of the magnetotail. Typical values of lobe properties ($B \approx 15$ nT and $n \approx 0.05$ cm^{-3}) yield a reconnection inflow speed of 150 km/s. In around 10 minutes, a typical timescale for the expansion phase of a substorm, about 15 R_e of magnetic flux in the lobes can reconnect.

Some studies have produced findings that at first glance appear to contradict these previous results. In studies of forced reconnection, where a tearing mode stable system is perturbed on the boundaries to drive reconnection, the authors found that the maximum reconnection rate scaled like $(d_i/L)^{3/2}$ (Ref. 26) and $(d_i/L)^{1/2}$,[27] and was also dependent on $k_p d_i$,[9] where L is the system size and k_p is the mode number of the forcing perturbation. A dependence on $k_p d_i$ is equivalent to a dependence on d_i/L in the thin current sheet studies discussed previously[17,23] and in this current study. In addition, in studies with a double current sheet with a large guide field the authors found that the timescales of reconnection depended on d_e/L and ρ_s/L, where $\rho_s = c_s/(eB_{z0}/m_i c)$, and c_s is the sound speed.[11,28] All of these studies, however, examine reconnection rates at times when $w \lesssim d_i$ and $w \lesssim \rho_s$,[9,11,26–28] where w is the magnetic island width and d_i and ρ_s define the length scales where the ions decouple from the reconnecting magnetic field. When the magnetic island is this small, the reconnected flux cannot fully couple to the ions, probably reducing their outflow velocity to less than the relevant Alfvén speed. In our view the period of time when the magnetic island is unable to fully couple to the ions should be considered as part of the developmental phase of reconnection. In addition, in these earlier studies the authors examined equilibria with system size equilibrium current sheets where the strong current sheet that forms in the dissipation region as reconnection develops is embedded inside of a much larger equilibrium current sheet. In such a system the magnetic field upstream of the dissipation region, B_d, changes significantly throughout the reconnection process. However, in none of these studies did the authors renormalize the reconnection rate using a value of B_d explicitly measured from the simulations. Two used values of B_d derived from analytical scaling arguments.[9,27] The rates of reconnection must be normalized to the value of B_d measured from the simulation data to unambiguously determine the scaling of reconnection in the case of embedded reconnection.

In order to prevent further misunderstanding, we clearly give the definitions used in discussing reconnection in this study. The "reconnection rate" is the instantaneous rate of

transfer of flux through the dissipation region, $E=(1/c)\partial\psi/\partial t$, and as such may change dramatically throughout the fast reconnection phase. We reiterate that the scaling of reconnection rates discussed in this paper do not include the developmental phase. The ''reconnection time'' is the time to reconnect a significant fraction of the available flux in the system and does not include the time required for the magnetic islands to grow to a large enough size to magnetize the ions. Alfvénic reconnection is defined as reconnection in which the aspect ratio of the ion dissipation region, $\delta/D\sim 0.1$, becomes independent of system size and the mechanism breaking the frozen-in constraint, i.e., the reconnection rate is only dependent on c_{Ad}. This reconnection rate is contrasted with resistive reconnection in the solar corona where $\delta/D\sim 10^{-7}$.

In many physical systems of interest the initial current layers have macroscopic extent and B_d should evolve in time. Thus, previous theories of fast reconnection based on thin equilibrium current sheets may not apply. In this study we seek to generalize those past studies of reconnection by simulating reconnection in a double current sheet configuration with a system size wide initial equilibrium current sheet. The simulations are performed using the two-fluid code F3D which includes the Hall term and electron inertia in Ohm's law. The difficulty with examining the reconnection rate in this system is that B_d is changing significantly during the reconnection process, and this magnetic field must be determined accurately in order to determine the scaling of the reconnection rate. In resistive MHD, the determination of B_d is relatively straightforward because the dissipation region has only one scale.[2] In collisionless plasmas, however, the dissipation region develops a two scale structure associated with the effective ion and electron Larmor radii,[23,29–31] which complicates the determination of B_d.

Any large scale reconnection process must strongly couple to the ions and the rate is therefore limited by the Alfvén speed. Because the ions play such an important role in controlling the reconnection rate, we use the ion dissipation region to determine δ, D, B_d and V_{out}, where δ and D are the width and length of the ion dissipation region, B_d is the magnetic field just upstream of the ion dissipation region, and V_{out} is the ion outflow from this dissipation region. Using the location where the ion and electron inflows decouple to define the edge of the ion dissipation region, we describe a procedure for rigorously determining B_d at a given time directly from the simulation results. After renormalizing the reconnection rate using this B_d, we find that for large enough systems, the aspect ratio of the ion dissipation region, δ/D, asymptotes to a constant value around 0.1. This value is independent of system size for cases in which a large fraction of the reconnection occurs for an island half width w that exceeds $5d_i$. This typically requires the equilibrium scale length L_y along the inflow direction to satisfy $L_y\geqslant 20d_i$. During this constant δ/D phase, which we call ''asymptotic reconnection,'' most of the island growth occurs and a large fraction of the magnetic flux is reconnected in a very short period of time. In contrast, the developmental phase of reconnection is quite long and the timescales involved depend strongly on d_i/L and other factors. A simple model for reconnection in this asymptotic phase is developed that yields timescales for explosive energy release roughly comparable to those seen in physical systems. We briefly discuss previous studies of the reconnection scaling and mention studies that could be done to allow a relevant comparison to the results of this paper.

In order for reconnection to reach the fast asymptotic phase, V_{out} must scale with c_{Ad} and the dispersive wave physics due to the Hall term (whistlers in this case) must begin to play a role inside the ion dissipation region to allow δ/D to approach a finite, steady value. We examine the developmental phase of reconnection in our simulations and make the following observations. In all cases V_{out} is significantly less than c_{Ad} during the developmental phase, although the disparity varies greatly depending on the value of the tearing mode stability parameter Δ'. The quantity Δ' is a measure of the energy release from reconnection. Small Δ' manifests itself as a back pressure that counteracts the magnetic tension force accelerating the ions away from the x-line. For the smallest Δ' simulations, these two competing forces are nearly equal, making V_{out} very small and causing an extremely long Rutherford-like developmental phase.[32,33]

In the larger Δ' cases, the transition to the asymptotic phase was accompanied by a decrease in the length of the ion dissipation region, D, which was facilitated by the rise in strength of the Hall term in Ohm's law. The onset of Hall physics inside the ion dissipation region is correlated with the decrease in width of the inner electron current sheet. The speed with which D decreases during this transition depends strongly on the strength of the inner electron current sheet. In cases with a relatively strong electron current sheet, D exhibits an almost step-like transition between the developmental and asymptotic phases. For weaker current sheets, D very gradually decreases.

II. SIMULATIONS

This study was performed using the two fluid F3D code, which is fully parallelized for the largest available computational platforms using 3D domain decomposition with Message Passing Interface (MPI). The Hall MHD equations stepped forward in time are:

$$\frac{\partial n}{\partial t}=-\nabla\cdot\mathbf{J}_i, \tag{1}$$

$$\frac{\partial \mathbf{J}_i}{\partial t}=-\nabla\cdot(\mathbf{J}_i\mathbf{J}_i/n)+\mathbf{J}\times\mathbf{B}-\frac{T}{n}\nabla n, \tag{2}$$

$$\frac{\partial \mathbf{B}'}{\partial t}=-\nabla\times\mathbf{E}', \tag{3}$$

$$\mathbf{E}'=\frac{\mathbf{J}}{n}\times\mathbf{B}'-\frac{\mathbf{J}_i}{n}\times\mathbf{B}, \tag{4}$$

$$\mathbf{B}'=(1-d_e^2\nabla^2)\mathbf{B},\quad \mathbf{J}=\nabla\times\mathbf{B}, \tag{5}$$

where $\mathbf{J}_i\equiv$ ion flux, $\mathbf{u}_e=(\mathbf{J}_i-\mathbf{J})/n=$ electron velocity, $d_e\equiv c/\omega_{pe}$, and $T\equiv T_i+T_i$ is the total temperature. The initial equilibrium consists of a system size double current sheet with the following magnetic field: $B_x=B_0\sin[2\pi(y+L_y/4)/L_y]$. The density at the center of the current sheets is

1.5 n_0 and falls to 1.0 n_0 so as to balance magnetic pressure. All of the initial current is carried by the electrons and the ions are initially at rest. Time has been normalized to $t_o = \Omega_i^{-1} = (eB_o/m_i c)^{-1}$. Length has been normalized to $L_o = d_i = c\sqrt{m_i/(4\pi n_o e^2)}$, with n_o equal to the minimum initial density in the system. The velocities therefore are normalized to the Alfvén velocity. We also assume quasineutrality: $n_i \approx n_e$. For this study, we have taken the isothermal approximation with $T=1.0$ so that the sound speed equals the Alfvén speed. In order to prevent energy buildup at the grid scale, we have included fourth order dissipation in each of the equations of the form $\mu_4 \nabla^4$, where $\mu_4 = 5.1 \cdot 10^{-5}$ unless states otherwise.

The above equations form a closed set. In Ohm's law in (4) the $\mathbf{J}/n \times \mathbf{B}'$ term produces the Hall effect and introduces the scale length $d_i \equiv c/\omega_{pi}$ into the equations. This scale does not appear explicitly because it has been absorbed into the normalization. The electron inertia, or electron mass, in Ohm's law manifests itself through the term proportional to d_e^2 in the definition of $\mathbf{B}'$. In normalized coordinates, $d_e = \sqrt{m_e/m_i}$ and is treated as a spatially constant free parameter. At the end of each time step, $\mathbf{B}$ is unfolded from $\mathbf{B}'$ using fast Fourier transforms.

The electron to ion mass ratio, m_e/m_i, is chosen to be 1/25, making $d_e = 0.2$. The 2D simulation domain consists of $n_x \times n_y$ grid points with the physical size $L_x \times L_y$, with boundaries at $x = \pm L_x/2$ and $y = \pm L_y/2$. The boundary conditions are periodic in all directions. Typical parameters for this system are 2048×512 grid points with a physical system size of 204.8×51.2. This produces grid scales $\Delta_x = \Delta_y = 0.1$, which is the default unless stated otherwise.

The system was seeded by an x-line in both current sheets to create the double tearing mode. These x-lines were formed by perturbing the equilibrium with $\tilde{\mathbf{B}} = \hat{\mathbf{z}} \times \nabla \tilde{\psi}$, where $\tilde{\psi} = b_{y0}(L_x/4\pi)\{1 + \cos[(y \pm L_y/4)4\pi/L_y]\}\sin(k_p x)$, where b_{y0} is a constant parameter, $k_p = 2\pi/L_x$ is the initial x-line perturbation mode, and the "$\pm$" is chosen for the appropriate current sheet. Note that the maximum perturbations $\tilde{B}_x$ and $\tilde{B}_y$ are $b_{y0}L_x/L_y$ and b_{y0}, respectively. The sign of $\tilde{\psi}$ is chosen to produce x-lines at $(x,z) = (\pm L_x/4, \mp L_y/4)$ and o-lines in the other quadrants. From this perturbation, an approximate initial value for the island half width is $w = (1/\pi)\sqrt{L_x L_y b_{y0}}$.

In order to provide symmetry breaking such that any small flux bubbles generated during reconnection will be ejected downstream, there was a very small amount of random noise added to the system. B_x and B_y were perturbed with Fourier modes to insure that $\nabla \cdot \mathbf{B} = 0$, with $|\tilde{B}_{\max}| \approx 10^{-4}$. The initial ion current was also perturbed with random fluctuations with $|\tilde{J}_{\text{imax}}| = 10^{-4}$.

III. RESULTS—GENERAL

Any study of the reconnection rate must address the structure of the dissipation region, i.e., the nonideal MHD region surrounding the x-line in which the magnetic field lines break and reform. A simple Sweet–Parker-like scaling argument yields insight into the reconnection process.[1,34,35] Continuity into and out of this region yields:

$$V_{\text{in}} \sim \frac{\delta}{D} V_{\text{out}}, \tag{6}$$

where V_{in} and V_{out} are the inflow and outflow velocities of the dissipation region, δ is the width of the dissipation region along y, and D is the length of the dissipation region along x. For simplicity we assume that reconnection is relatively steady during the transit time of ions through the dissipation region. The ion force equation along x yields $m_i n V_x (\partial V_x/\partial x) \sim B_y (\partial B_x/\partial y)/4\pi$. Using $\nabla \cdot \mathbf{B} = 0$, one obtains $V_{\text{out}}^2 \sim B_d^2/(4\pi m_i n)$, where B_d is the magnetic field at the inflow edge of the dissipation region.[1] Finally, V_{in} is determined by the $E \times B$ drift speed into the dissipation region, yielding $V_{\text{in}} \sim cE_z/B_d$, which gives

$$cE_z \sim \frac{\delta}{D} \frac{B_d^2}{\sqrt{4\pi m_i n}}. \tag{7}$$

The two most important factors in Eq. (7) are B_d and δ/D. Although the density can and does change in time, in these simulations it changes at most from $n=1.5$ to $n=1.0$, which leads to only a 20% change in the reconnection rate. Over the times of interest in these simulations, E_z varies by a factor of over 20. Thus, in the remainder of the discussion we will ignore the effects of density variation. B_d gives a measure of the amount of magnetic free energy that can drive reconnection at any given time. δ/D is the critical geometric ratio that has been the subject of intense scrutiny because it plays such an important role in determining the reconnection rate.

TABLE I. Simulation information.

Run #	$L_x \times L_y$	Δ	b_{y0}	w_0	t_*	w_*
1	102.4×51.2	0.1	$6.8 \cdot 10^{-4}$	0.55	28 000	7.4
2	204.8×51.2	0.1	$3.5 \cdot 10^{-4}$	0.55	3320	6.1
3	409.6×51.2	0.1	$1.8 \cdot 10^{-4}$	0.55	4200	8.0
4	409.6×102.4	0.1	$8.8 \cdot 10^{-5}$	0.55	20 040	9.9
5	102.4×25.6	0.1	$3.5 \cdot 10^{-4}$	0.25	⋯	⋯
6	51.2×12.8	0.1	$8.8 \cdot 10^{-5}$	0.05	⋯	⋯
7	102.4×25.6	0.05	$3.0 \cdot 10^{-4}$	0.28	⋯	⋯

Table I shows information on the seven simulations used for this study, showing run number, physical system size ($L_x \times L_y$), grid scale (Δ), initial x-line perturbation magnitude (b_{y0}), initial island half width (w_0), time at beginning of asymptotic phase (t_*), and island half width at beginning of asymptotic phase (w_*). The cases that did not exhibit a clear asymptotic phase are marked with a "⋯."

In order to examine the scaling of the reconnection rate versus the system size, we ran several reconnection simulations with different system sizes. Note that in our simulations, the initial x-line perturbation scale length is $k_p = 2\pi/L_x$. The raw reconnection rates, $E_r = \partial\psi/\partial t$, versus time are shown in Fig. 1 for the four largest simulations (Runs 1–4). These reconnection rates are determined by taking the time derivative of the difference in ψ between the

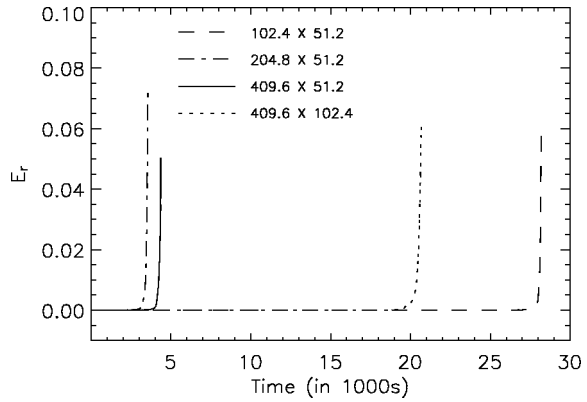

FIG. 1. Reconnection electric field versus time for four different system sizes (runs 1–4).

x-line and o-line. No data are shown after the magnetic islands begin to strongly affect the x-lines above and below them. The most striking feature of these simulations is the very long developmental phase compared to the fast reconnection phase. All of the simulations have a very long phase of almost no reconnection, and then a sudden acceleration of reconnection at late time. The length of the developmental phase clearly depends strongly on L_x and L_y. Because B_d is increasing during the duration of the simulation, the reconnection rate never reaches a steady value, which makes comparing the late time reconnection rates between these runs quite difficult.

An example of the structure of the ion dissipation region during the developmental and asymptotic phases is shown in Fig. 2 for the 409.6×102.4 run (run 4): (left column) developmental phase at $t=9500$, (right column) asymptotic phase at $t=20496$. The x and y axes have been shifted to locate the x-line at (0,0), and the lower left quadrant of the simulation is shown: Figures 2(a) and 2(b) J_z, the out-of-page current; Figs. 2(c) and 2(d) J_{iz}, the ion out of page current; Figs. 2(e) and 2(f) V_{ix}, the ion outflow; and Figs. 2(g) and 2(h) B_z, the out-of-plane magnetic field. In Fig. 2(b) the color bar has been skewed to show detail downstream of the x-line. During the developmental phase the system clearly shows a long thin Sweet–Parker dissipation region reminiscent of MHD reconnection with a constant resistivity. The ion outflows are

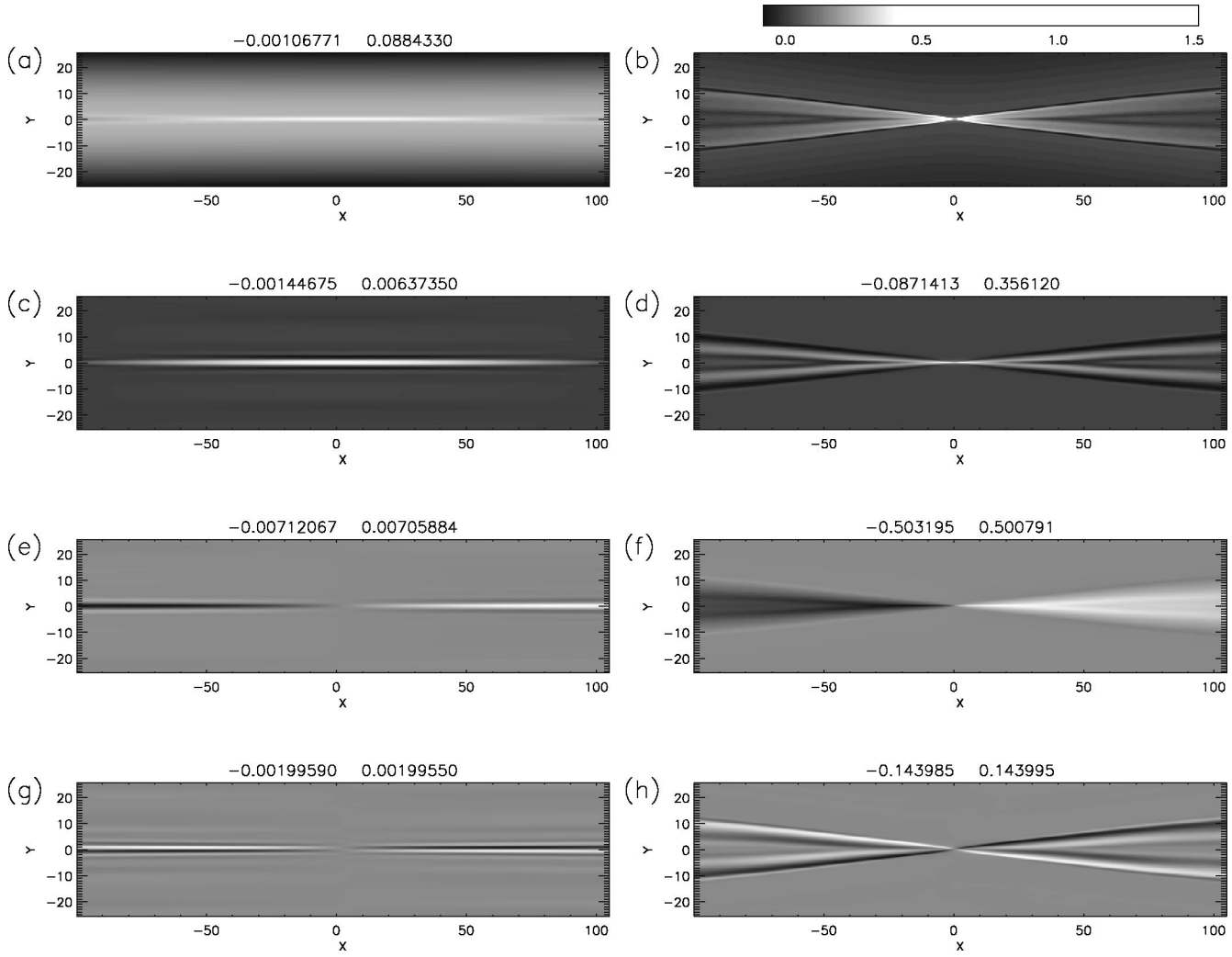

FIG. 2. Developmental and asymptotic phases for the 409.6×102.4 (run 4) simulation. The x and y axes have been shifted to locate the x-line at (0,0) and only the lower left quadrant of the simulation is shown. (left column) Developmental phase at $t=9500$ (right column), asymptotic phase at $t=20\,496$. (a) and (b) J_z, out-of-page current; (c) and (d) J_{iz}, ion out of page current; (e) and (f) V_{ix}, ion outflow; (g) and (h) B_z, out-of-plane magnetic field. The numbers at the top of each figure are the minimum and maximum values. In (b) the color bar has been skewed to show detail downstream of the x-line.

collimated into a long and thin region, which severely throttles the reconnection rate. B_z associated with the Hall term is very small, with $B_{z\,\max}\approx 0.002$ compared to $B_d \approx 0.1$, where the procedure for determining B_d will be described later. Note that the maximum magnetic field in the system is $B_0 = 1.0$. The reconnection rate is also limited at this time because $V_{\text{out}} \ll B_d$. The asymptotic phase in the right column shows the usual properties associated with fast Hall-mediated reconnection. The long thin current sheet, as well as the ion current, has opened out into an x-point or cross-shaped structure. The ion outflows also broaden out, which removes the throttling effect on the ions. At this time $B_d \approx 0.37$, so $B_{z\,\max}$ is a significant fraction of B_d and $V_{\text{out}} \sim B_d$.

Recent satellite observations have revealed bifurcated current sheets in the magnetotail with increasing frequency.[36–39] Although some of these cases are not associated with reconnection, a bifurcated current sheet is one of the signatures of fast reconnection, e.g., see the bifurcated current sheet located just downstream of the x-line in Fig. 2(b). There are bands of current primarily carried by the electrons located just downstream of the separatrices. Associated with these bands of current are the B_z perturbation due to the Hall term, a weak ion current, and the ion outflow just downstream.

IV. ASYMPTOTIC PHASE

In any system where the magnetic field just upstream of the dissipation region is changing during reconnection, it is necessary to carefully determine that magnetic field B_d. Without normalizing to the Alfvén speed based on this value, it is impossible to make meaningful comparisons of the instantaneous reconnection rate between different simulations or to even understand the time changing rate of reconnection in a single simulation. In resistive MHD systems, it is quite straightforward to determine the upstream magnetic field B_d because reconnection usually forms a long current sheet that is clearly of the Sweet–Parker form.[2,6,33] However, in whistler mediated reconnection, the ion dissipation region has two inner scales, complicating the matter significantly: d_i the scale where the ions decouple from the magnetic field, and d_e the scale where the electrons decouple from the magnetic field. We have developed a procedure for determining B_d, δ, D, and V_{out} from the simulation data for any generic reconnecting system.

We find that the simulations exhibit a fast asymptotic reconnection phase during which $\delta/D \sim 0.1$, independent of system size (L_x and L_y). The time of the beginning of the asymptotic phase is also the time when V_{out} begins to scale with B_d, although it is unclear if this behavior is generic. In addition, at the beginning of the asymptotic phase $w \geqslant 5d_i$, where w is the magnetic island width. During the asymptotic phase for the largest simulation in this study (409.6×102.4, run 4), 75% of the island growth and 90% of the magnetic flux reconnection occurred, even though this phase only lasts for 3% of the simulation time.

Any large scale reconnection process must strongly couple to the ions and as such is limited by the Alfvén speed.

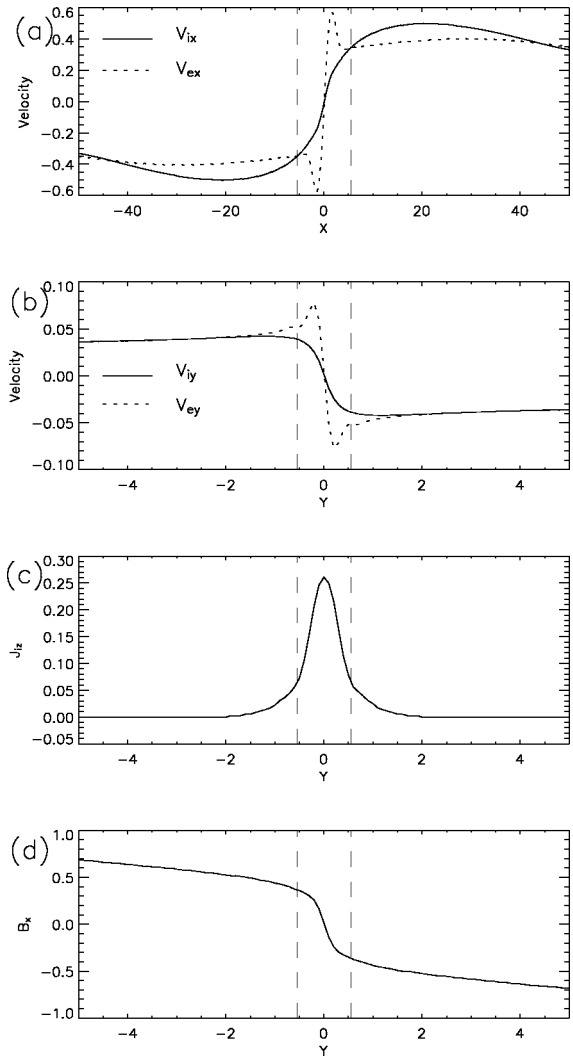

FIG. 3. Determining the ion dissipation region parameters. The 409.6×102.8 case (run 4) at $t = 20\,496$. The axes have been shifted so that the x-line is located at (0,0). (a) Outflow velocities along x at $y = 0$, (b) inflow velocities along y at $x = 0$, (c) J_{iz}, ion out-of-plane current, (d) B_x. The vertical dashed lines in (b)–(e) denote the edges of the dissipation region. For this time in this particular run, $\delta = 0.55$, $B_d = 0.37$, $D = 5.5$, and $V_{\text{out}} = 0.35$.

Because the ions play an important role in controlling the reconnection rate, we use the ion dissipation region to determine δ, D, B_d, and V_{out}. We define the ion dissipation region as the region where the ion flows decouple from the magnetic field. Plotted in Fig. 3 are slices of data for the 409.6×102.4 case (run 4) at the same time as the right column in Fig. 2. The slices are used to determine the physical boundaries of the ion dissipation region, which are shown as vertical dashed lines. V_{out} is determined by examining a cut through the x-line along the x direction of V_{ix} and V_{ex}, as shown in Fig. 3(a). The electron velocity very quickly spikes up to a large velocity inside the whistler dominated part of the ion dissipation region. As the electrons approach the edge of the ion dissipation region, they must slow down to flow roughly with the ions. We define the downstream edge of the ion dissipation region as the location where the electron and ion velocities cross, and D is the distance from the x-line to

this location. Besides the theoretical motivation, we chose this crossing point as opposed to the location of maximum ion flows because the location of maximum ion flow tends to move downstream at late time. During the developmental phase, however, $|V_{ix}|$ reaches its maximum value before $V_{ix}=V_{ex}$, so during that time the downstream edge of the dissipation region is located where V_{ix} is maximum. V_{out} is set equal to V_{ix} at the downstream edge of the dissipation region. There are two values corresponding to the two downstream–upstream edges of the dissipation region. These are averaged to obtain the final value. From Fig. 3(b) we find that at this particular time, $D=5.5$, and $V_{\text{out}}=0.35$.

The upstream edge of the ion dissipation region is determined by the location where the ion and electron inflows diverge. Figure 3(b) shows a cut of V_{iy} and V_{ey} through the x-line along y. The electrons and ions flow together towards the x-line until about $2c/\omega_{pi}$ upstream of the x-line, where the electrons begin to accelerate towards the x-line. Determining a clear point to call the upstream edge of the dissipation region was difficult because the electron have a long ''tail'' where they are still roughly flowing with the ions. The non-MHD region, however, is clearly defined by J_{iz} [Fig. 3(c)], which is normally neglected in MHD but becomes nonzero when the ions decouple from the magnetic field and are accelerated along z by the reconnection electric field. The upstream edge of the dissipation region was determined by taking the location where the ion current is 25% of its maximum value, which is denoted by the dashed lines. The width of the dissipation region, δ, is set equal to the distance from the upstream edge of the dissipation to the x-line. B_d is equal to the magnetic field at this upstream edge of the dissipation region, as shown in Fig. 3(d). At this particular time, $\delta=0.55$ and $B_d=0.37$.

The ion dissipation region parameters that have been determined from this procedure are plotted versus time for the 409.6×102.4 case (run 4) in Fig. 4: (a) B_d, (b) V_{out}, (c) δ, and (d) D. The vertical dashed line represents the beginning of the asymptotic phase and the time at which $V_{\text{out}}\propto B_d$ as determined from Fig. 5(a). B_d and V_{out} change very little during the developmental phase and then suddenly increase sharply. δ and D decrease sharply just prior to the asymptotic phase and remain relatively constant thereafter. The sharp decrease in D is associated with the activation of the Hall term in Ohm's law and the rise of whistler physics inside the dissipation region, which will be discussed in Sec. V.

A quick glance at the ion dissipation region parameters determined from Fig. 3 shows that they are consistent with $V_{\text{out}}\sim B_d$ and $\delta/D\sim0.1$. Figure 5 shows the results of this scaling study for several different L_x and L_y (runs 1–4). Plotted are (a) V_{out} versus B_d, (b) E_r versus B_d, and (c) E_r versus B_d^2. All simulations were perturbed with an initial half island width of 0.55.

Ignoring the small variations in density and renormalizing to code units, the Sweet–Parker-like analysis leading up to Eq. (7) yields $V_{\text{out}}\sim B_d$ and $E_r/B_d^2\sim\delta/D$. The scaling of V_{out} with B_d must be satisfied if a Sweet–Parker-like analysis is to be valid, which is shown in Fig. 5(a). By the time $B_d=0.3$, all of the simulations show clearly that $V_{\text{out}}\propto B_d$. The diamond on each curve represents the point at which

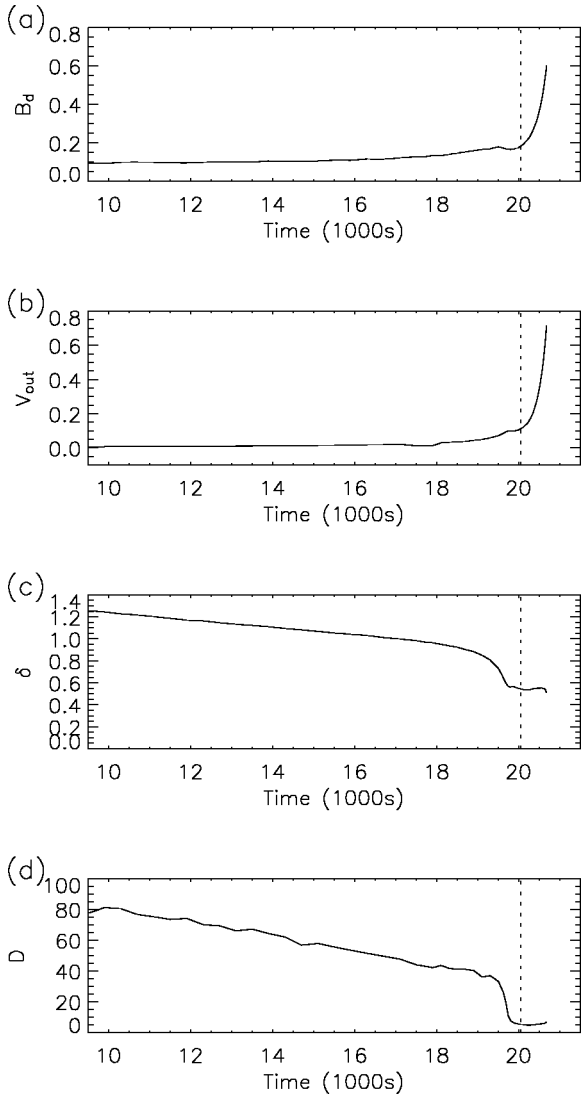

FIG. 4. Ion dissipation region parameters for the 409.6×102.4 case (run 4) versus time: (a) B_d, (b) V_{out}, (c) δ, and (d) D. The vertical dashed line represents the beginning of the asymptotic phase and the time at which $V_{\text{out}}\propto B_d$ as determined from Fig. 5(a).

V_{out} begins to scale with B_d. All of the simulations except 102.4×51.2 (run 1) show a clear kink just before the diamond. This kink is associated with the sudden ''opening out'' of the current sheet to form an x-point structure where D is independent of L_x and L_y. The 102.4×51.2 case does not show this kink because before the asymptotic phase the system exhibits Rutherford reconnection, in which D is probably independent of L, but V_{out} is quite small compared to B_d.

Figures 5(b) and 5(c) show the scaling of E_r versus B_d and B_d^2. Bear in mind that the diamonds indicate the time at which the scaling becomes trustworthy because $V_{\text{out}}\propto B_d$. Examining the post-diamond data, E_r clearly does not scale with B_d because the slope of the lines for $B_d<0.3$ is significantly less than it is for $B_d>0.3$. E_r versus B_d^2, on the other hand, shows a constant slope over a large range of B_d^2, independent of L_x, and L_y. Note that diamonds in Fig. 5(c) approximately delineate the time when the slope of each line

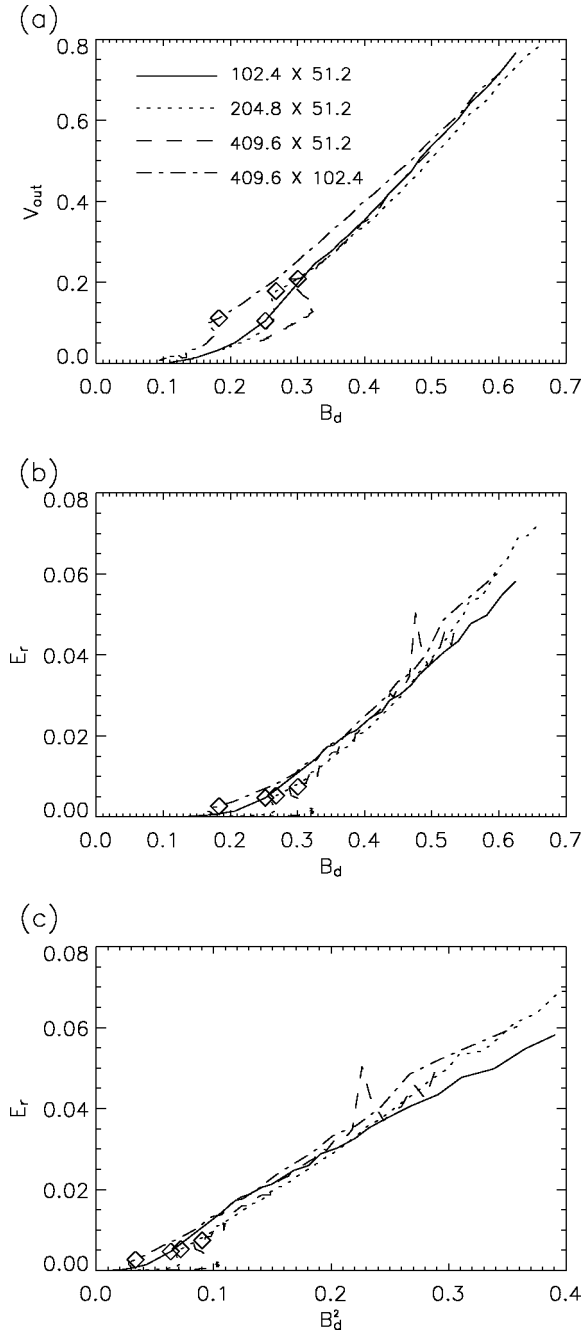

FIG. 5. Scaling of reconnection for runs 1–4. The diamonds denote the time when V_{out} begins to scale proportionally with B_d, which is coincident with the beginning of the asymptotic phase for these simulations.

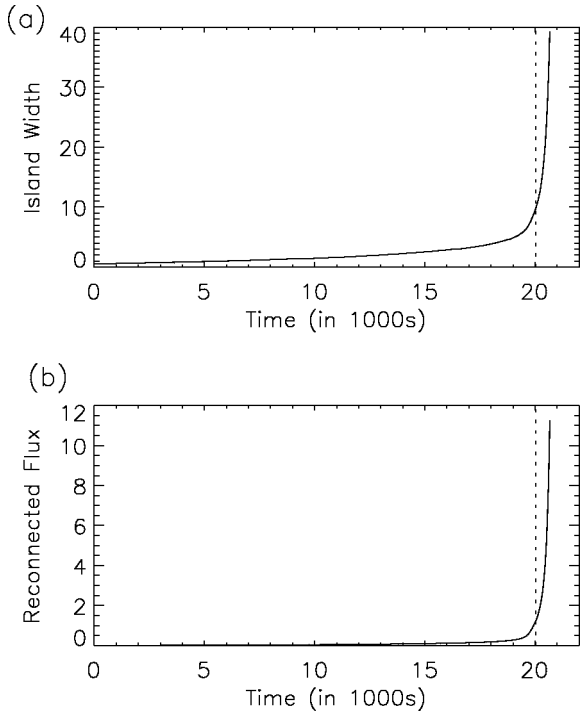

FIG. 6. Island width and reconnected magnetic flux versus time for the 409.6×102.4 simulation (run 4). The dashed line denotes the transition between the developmental and asymptotic phases.

becomes relatively constant. In this set of simulations, the transition to the asymptotic phase occurs at roughly the same time that V_{out} becomes proportional to B_d, but it is not clear if this is a generic phenomenon. The localized spike in E_r for the 409.6×51.2 case (run 3) is caused by the adjustment of the system to a secondary island that formed at one of the x-lines at an earlier time. The average slope of the lines in Fig. 5(c) is about 0.18, which corresponds to δ/D and V_{in}/c_{Ad} of about 0.1. For the largest simulation, 409.6 ×102.4 (run 4), the developmental phase lasts from $t=0-20\,040.0$, and the asymptotic phase lasts from $t=20\,040.0$ to $t=20\,672.0$. Although the asymptotic phase only lasts for a very short period of time, most of the island growth and energy release happens during this phase, as shown in Fig. 6. The dashed line is at $t=20.040\cdot 10^3$. Roughly 75% of island width growth and 90% of the magnetic flux occurs during the asymptotic phase, even though this phase only lasts for 3% of the simulation time. This dominance of the asymptotic phase will not be modified substantially by changing the magnitude of the initial x-line perturbation, b_{y0}. Preliminary studies indicate that w_* may in fact be independent of b_{y0} for $w_0<3c/\omega_{pi}$. If w_* scales solely with the microscales in the system, for larger system sizes we would expect that even higher percentages of flux reconnection would occur in the asymptotic phase. During this entire phase the scaling $V_{in}\approx 0.1\ c_{Ad}$ remains valid even though B_d changes by more than a factor of 3.

Although most of the island width growth occurs during the asymptotic phase of reconnection, the island width w is still substantial at the time of the transition to asymptotic reconnection, as is listed in Table I. For all of the systems that show clear asymptotic scaling, this transition occurs for $w\geqslant 5\,d_i$. Unless $w\gg d_i$, the ions are not completely magnetized within the magnetic islands and ion acceleration in the outflow direction cannot reach the expected values, i.e., V_{out} does not scale with B_d.

The independence of δ/D from L_x and L_y during the asymptotic phase is consistent with previous studies of the scaling of the reconnection rate in systems with initial equilibrium current sheets with a thickness $\sim d_i$.[17] These studies found that the key factor allowing δ/D to become independent of system size was the dispersive nature of the physical waves present in the outer regions of the ion dissipation

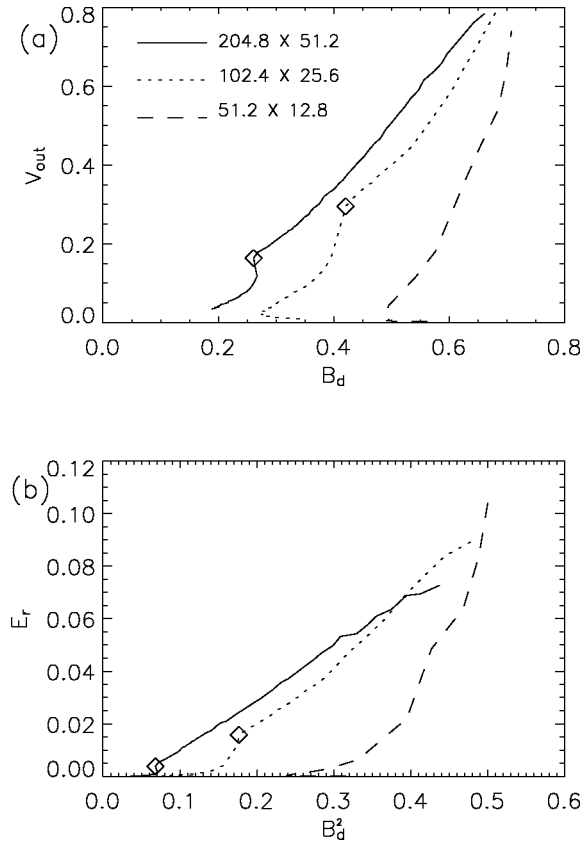

FIG. 7. Reconnection scaling for relatively small simulations (runs 2,5,6). The diamonds denote the time when V_{out} begins to be roughly proportional to B_d.

region.[17,23,25] Due to the Hall term, the dissipation region develops a two scale structure. An outer region where the electrons are frozen-in but the ions are not, and a very small inner scale where the electrons finally decouple from the magnetic field. In this outer region, the bent field lines usually respond as either whistlers in the case with no B_{z0}, or as kinetic Alfvén waves in the case with a large B_{z0}. Both of these waves have $\omega \propto k^2$, which means that $V \propto k$. This dependence of V on k allows the cross-shaped current sheet structure associated with $\delta/D \sim 0.1$ to be stable. In the MHD case with constant resistivity, on the other hand, this cross-shaped current quickly collapses down to form a long thin Sweet–Parker current sheet.[2,33,40]

In addition, these studies of Hall mediated reconnection in thin current sheets found that the reconnection rate was independent of the process which finally breaks the frozen-in condition on the electrons, m_e/m_i, again due to the dispersive nature of the whistler waves.[18–20,23] Although, it has not been explored in this study, we expect that the asymptotic reconnection rate is also independent of m_e/m_i.

When studying the scaling of the reconnection rate as applicable to large systems where $L \gg d_i$ it is imperative to make the system size large enough. If the system is not large enough, the non-MHD dispersive waves begin to impact the dynamics of the system size scales. Figure 7 shows V_{out} versus B_d and E_r versus B_d^2 for a set of smaller simulations (runs 2,5,6). The two largest simulations show rough scaling of V_{out} with B_d, with the location of the onset of this scaling marked with a diamond. It is questionable whether the smallest simulation ever exhibits linear scaling, and the 102.4 $\times$25.6 case is also marginal. The slope of E_r versus B_d^2 definitely changes as L_y decreases from 25.6 to 12.8. The $L_y = 51.2$ and 25.6 cases marginally scale the same, although near the end of the simulation the reconnection rate of $L_y = 25.6$ increases. The smallest simulation, however, does not show any clear scaling, with the slope of the curve increasing as the reconnection proceeds. This breakdown of this Sweet–Parker-like analysis is consistent with the system transitioning from an MHD dominated reconnection process to an electron MHD dominated reconnection process. Two previous studies examining the reconnection of flux bundles found that the scaling of the reconnection rate showed a clear kink when the distance between the two reconnecting flux bundles or islands was around 10 d_i.[6,41] This roughly corresponds to the $L_y = 25.6$ case, where the distance between the two reconnecting current sheets is 12.8.

V. DEVELOPMENTAL PHASE

In order for reconnection to reach an asymptotic phase when δ/D is independent of system size, there are two main requirements. One, the outflow speed must become comparable to the upstream Alfvén speed. And two, the dispersive wave physics due to the Hall term (whistlers in this case) must begin to control the dynamics inside the dissipation region.

A necessary condition for $V_{out} \propto c_{Ad}$ is an unimpeded tension force accelerating the ions away from the x-line, as was shown in the derivation of Eq. (7). The tearing mode stability parameter Δ' can shed some light on the scaling of this outflow speed, where $\Delta' = (\tilde{\psi}'(y \to 0+) - \tilde{\psi}'(y \to 0-))/\tilde{\psi}(y=0)$ and where the prime denotes a derivative along y. For the simulations in this study,[42]

$$\frac{\Delta'}{k_{y0}} = 2\sqrt{1-\frac{L_y^2}{L_x^2}}\tan\left(\frac{\pi}{2}\sqrt{1-\frac{L_y^2}{L_x^2}}\right), \tag{8}$$

where $k_{y0} = 2\pi/L_y$. Δ' is a measure of the field line bending stabilization of reconnection. When $\Delta' = 0$, the energy released from reconnection is perfectly balanced by the energy it takes to bend the field lines upstream of the x-line, and the tearing mode does not grow. When $\Delta' > 0$, reconnection can release energy and the tearing mode is unstable.[10] The field line bending stabilization of the tearing mode manifests itself as a total pressure gradient (∇P_{tot} with $P_{tot} = P + B^2/2$) opposing the tension force accelerating the plasma away from the x-line.

In a recent study the role of Δ' in resistive MHD simulations of reconnection was investigated.[33] The authors found that for all but very small values of Δ', the reconnection process exhibited Sweet–Parker scaling, with D increasing as Δ' increased. For very small Δ', however, the system evolved as predicted by Rutherford's quasi-static reconnection model.

In our system we see both scalings during the developmental phase. Figure 8 shows results for two different sys-

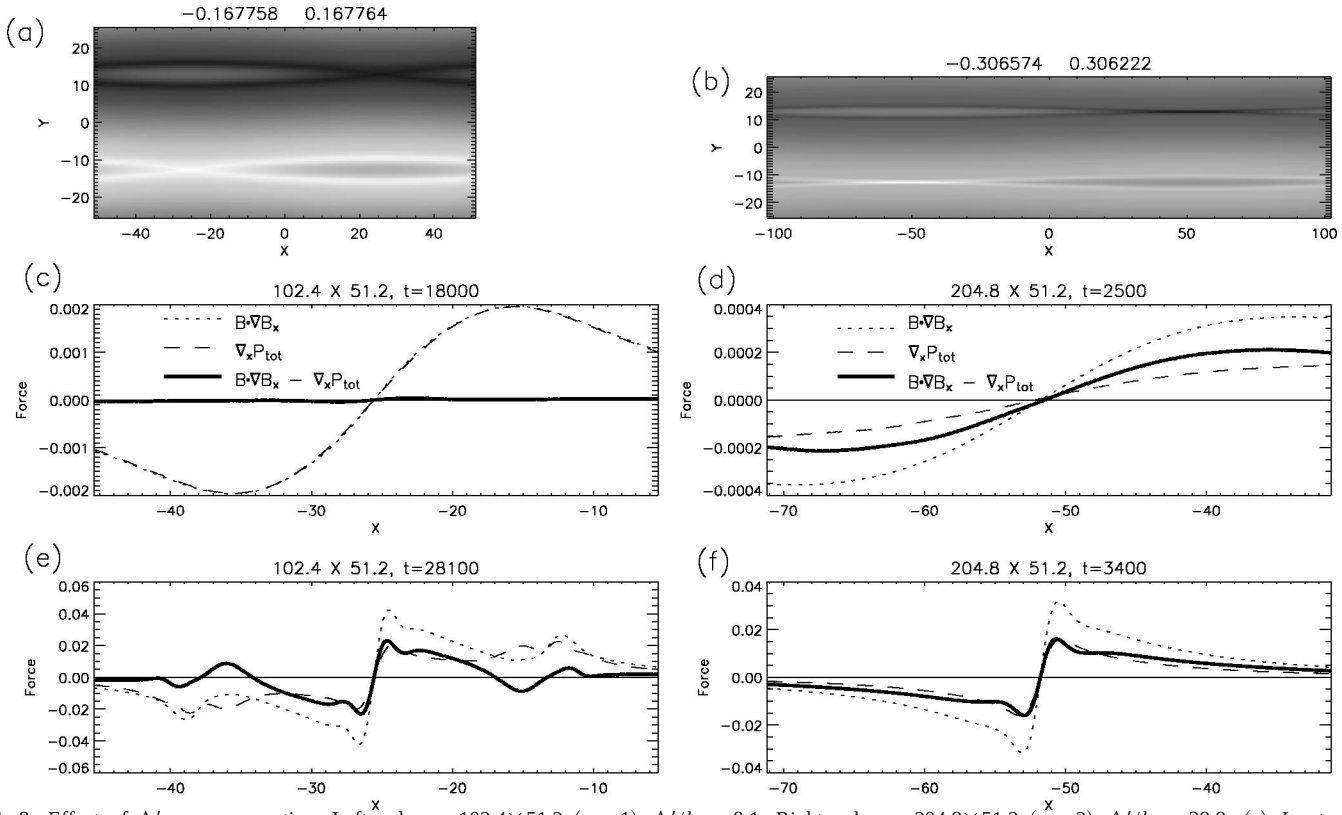

FIG. 8. Effect of Δ' on reconnection. Left column: 102.4×51.2 (run 1), $\Delta'/k_{y0}=8.1$, Right column: 204.8×51.2 (run 2), $\Delta'/k_{y0}=38.8$. (a) J_z, $t=18\,000$, (b) J_z, $t=2500$, (c) and (d) Developmental phase: Cut through x-line at $y=-12.8$ of outflow forces, (e) and (f) Asymptotic phase: Cut through x-line at $y=-12.8$ of outflow forces. The numbers above each grayscale plot are the minimum and maximum values.

tems: (left column) 102.4×51.2 (run 1), $\Delta'/k_{y0}=8.1$, and (right column) 204.8×51.2 (run 2), $\Delta'/k_{y0}=38.8$. At first glance from the grayscale plots of J_z in Figs. 8(a) and 8(b), the small Δ' system appears to have faster reconnection because the current sheet has opened out to form an x-structure. Figure 8(b), on the other hand, clearly has an elongated Sweet–Parker current sheet. Examining the forces in the x direction in a cut along x through the x-line at $y=-12.8$, Figs. 8(c) and 8(d), reveals an important difference between the simulations. The smaller Δ' case has $\mathbf{B}\cdot\nabla B_x \approx \nabla_x P_{\mathrm{tot}}$ so that V_{out} and the reconnection rate are extremely small. This is consistent with the very long duration of the developmental phase for run 1 shown in Fig. 1. After the transition to the asymptotic phase, as shown in Figs. 8(e) and 8(f), the scaling of $\mathbf{B}\cdot\nabla B_x$ and $\nabla_x P_{\mathrm{tot}}$ downstream of the x-line is very similar for the two Δ' cases. Most of the ion acceleration in the outflow direction occurs within about $10d_i$ of the x-line. In that region there is clearly a substantial total force roughly comparable in size to the tension force.

However, an unimpeded tension force is a necessary but not sufficient condition to have $V_{\mathrm{out}}\sim c_{\mathrm{Ad}}$. All of the simulations in Fig. 5 basically have an unimpeded outward tension force during the developmental phase except the 102.4 ×51.2 case (run 1), but V_{out} is much less than B_d in every case during this phase. To give some explicit values, for the times shown in Fig. 8, the 102.4×51.2 case (run 1) has $B_d=0.11$ and $V_{\mathrm{out}}=0.003$, and the 204.8×51.2 case (run 2) has $B_d=0.19$ and $V_{\mathrm{out}}=0.035$. Both cases clearly have $V_{\mathrm{out}} \ll B_d$, although the small Δ' case shows the most disparate values.

The transition to fast reconnection in all cases is therefore characterized by a sudden increase in V_{out} to make $V_{\mathrm{out}}\propto c_{\mathrm{Ad}}$. In the cases with relatively large Δ' this transition to the asymptotic phase is also accompanied by a decrease in the length of the dissipation region, D, and thus an increase in the dissipation region aspect ratio, δ/D. For the remainder of this section, we limit our discussion to the large Δ' cases.

Examining in detail the morphology of the developmental phase for the larger Δ' cases yields some interesting insights. Figure 9 shows a typical developmental phase for a high resolution run of size 102.4×25.6 (run 7) with $\Delta'/k_{y0}=38.8$ with a grid scale of 0.05 and $\mu_4=5.0\cdot 10^{-7}$: (a) Reconnection rate, (b) J_z at $t=450$, (c) J_z at $t=750$, and (d) J_z at $t=960$. At $t=450$, a clear system size length Sweet–Parker current sheet has formed with a scale length consistent with the initial perturbation scale length. The reconnection, of course, is extremely slow at this time. This current sheet gradually decreases in length as the reconnection proceeds and D decreases in length. At $t=960$, the current sheet has opened out to produce the x-point geometry associated with fast reconnection and D is a small fraction of the system size.

Figure 10 shows a more quantitative view of the morphology of the developmental phase in terms of the length of the dissipation region, D. Figures 10(a) and 10(b) shows D

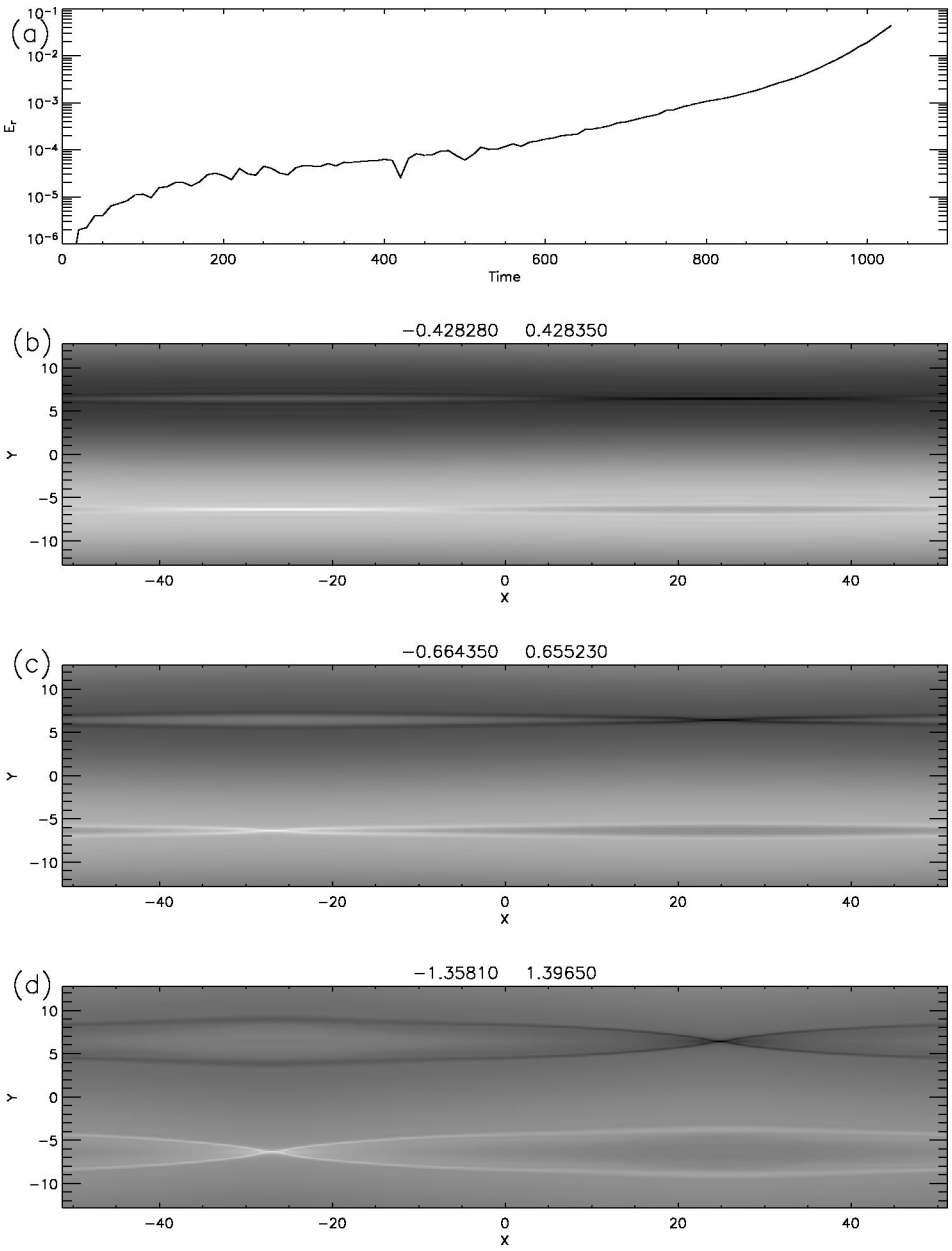

FIG. 9. The developmental phase of reconnection for run 7, (a) Reconnection rate (semilog plot), (b) J_z, $t=450.0$, (c) J_z, $t=750.0$, (d) J_z, $t=960$. The numbers above each gray-scale plot are the minimum and maximum values.

versus time for two different simulations: (left column) 204.8×51.2 (run 2), (right column) 102.4×25.6 (run 7). The decrease in the length of D for large Δ' cases is facilitated by the dispersive nature of whistler waves that arise due to the Hall term in Ohm's law.[17,23,25] In the case without a guide field, these waves are whistlers. The z component of Ohm's law along the outflow direction at the center of the current sheet is

$$cE_z=\left(-V_{ix}+\frac{J_x}{ne}\right)B_y, \tag{9}$$

where we have ignored electron inertia and dissipation and the approximation is valid near the center of the current sheet where B_xV_y is small. A good indicator of the relative strength of the Hall effect in reconnection can be made by comparing V_{ix} with $J_x/(ne)$. Figures 10(c) and 10(d) show the relative size of these two terms versus time. At each point in time, a cut through the x-line along x is examined and the point where $|J_x/ne|$ is maximum is found. Then this value is divided by V_{ix} at the same point and plotted. When $J_x/(nV_{ix})\approx1$, the Hall term is of equal strength to the $\mathbf{V}_i\times\mathbf{B}$ term. The sudden drop in D in Fig. 10(a) occurs around $t=3250$ when $J_x/(nV_{ix})\approx2$. The case on the right hand side reaches $J_x/(nV_{ix})\approx2$ at around $t=250$, very early on in the simulation, after which D again decreases although in this case more gradually.

The rise in strength of the Hall term occurs because of the decrease in width in the y direction of the electron dissipation region. The electron dissipation region is denoted by an intense perturbation current sheet carried almost exclusively by the electrons. We determine the width of the electron dissipation region, δ_e, by evaluating the perturbed current $\tilde{J}_z=J_z-J_{z0}$ in a cut along y through the x-line. The width at half max is doubled to yield δ_e (the total current sheet width equals $2\delta_e$). The values of δ_e versus time are

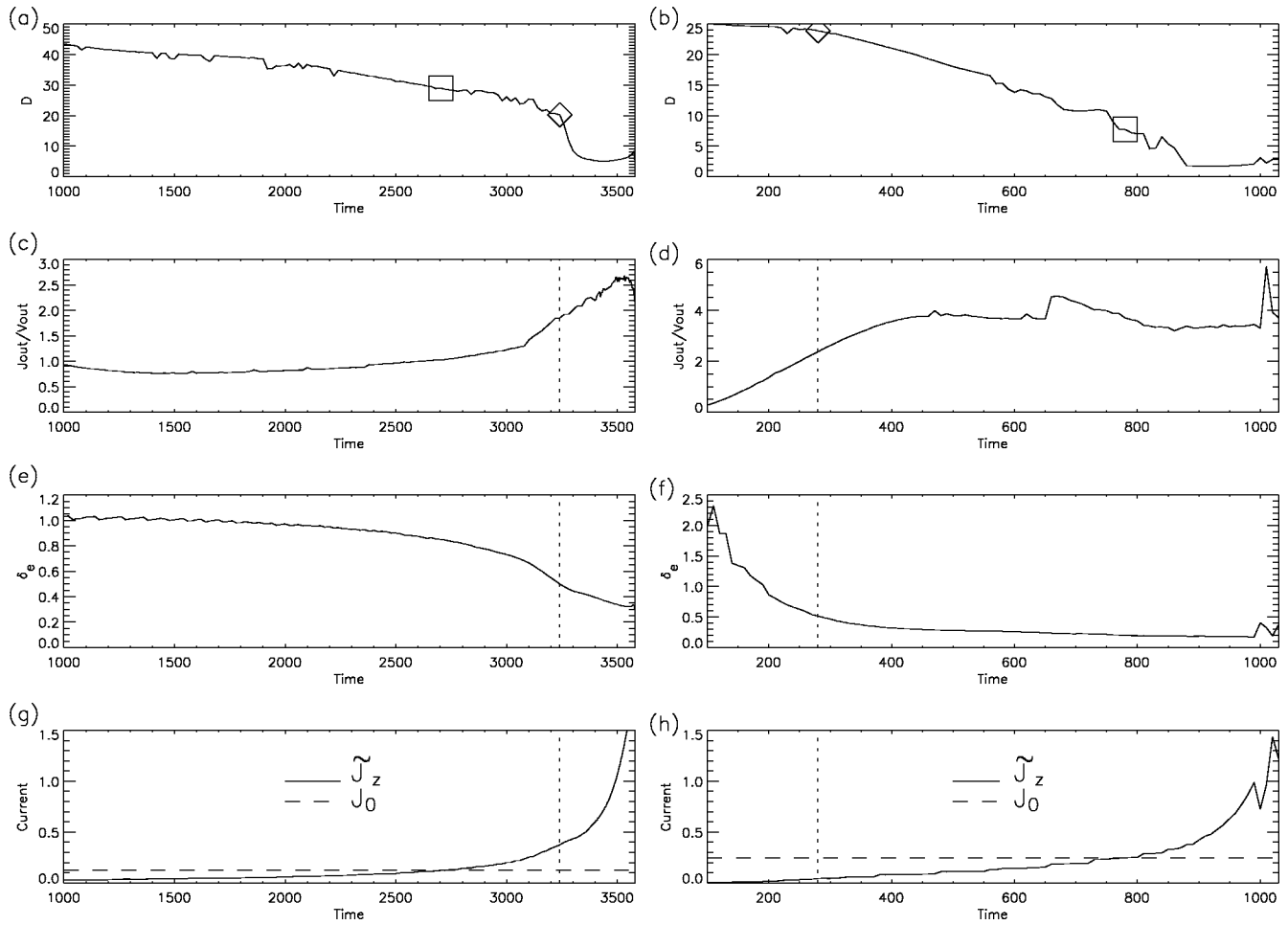

FIG. 10. Necessary conditions to accelerate the reconnection rate to the asymptotic phase: Results from an analysis of the ion and electron dissipation region. (left column) 204.8×51.2 (run 2), grid scale=0.1, (right column) 102.4×25.6 (run 7), grid scale=0.05. (a) and (b) Length of the dissipation region D, (c) and (d) $|J_x/V_{ix}|_{\max}$ versus time, where $|J_x/V_{ix}|_{\max}$ is the maximum value in a cut along x taken through the x-line, (e) and (f) width of the electron dissipation region, δ_e, (g) and (h) the average current inside the electron dissipation region, $\tilde{J}_z$, and the average equilibrium current J_{z0}. In (a) and (b), the shapes denote the times at which certain conditions are satisfied: (square) $\tilde{J}_z=J_{z0}$, (diamond) $\delta_e\approx 0.5$. In (c)–(h), the dotted vertical line denotes the time when $\delta_e=0.5$.

shown in Figs. 10(e) and 10(f). The 204.8×51.2 case (left column) satisfies $\delta_e=0.5$ around $t=3250$ whereas the 102.4×25.6 case (right column) satisfies $\delta_e=0.5$ very early in the simulation. The time when $\delta_e=0.5$ is denoted by diamonds. Both simulations show decreases in D after $\delta_e=0.5$. A significant increase in the reconnection rate when δ_e becomes smaller than the effective ion Larmor radius has been observed in previous 2D full particle[43] and two-fluid[44] simulations of forced reconnection.

A simplistic linear analysis of bent field line waves reveals the transition from Alfvén waves to whistler waves. Linearizing the continuity equation, the ion equation of motion, Faraday's law, and assuming $\mathbf{k}\|\mathbf{B}_0$ and incompressibility yields the following dispersion relation:

$$\left(\omega-\frac{k^2}{\omega}c_A^2\right)^2=k^4d_i^2c_A^2. \tag{10}$$

Solving for ω yields $\omega=c_A/(2\,d_i)[\pm k^2d_i^2 \pm kd_i\sqrt{k^2d_i^2+4}]$, where the two "±" are independent of each other. Taking both plus signs for simplicity, this equation yields $\omega=kc_A$ for $kd_i\ll 1$ and $\omega=k^2d_ic_A$ for $kd_i\gg 1$. The transition from the Alfvén wave to the whistler can be calculated by measuring $\alpha=d\ln\omega/d\ln k$ and noting that at any given k, $\omega\propto k^\alpha$. A plot of α is shown versus kd_i in Fig. 11. As expected $\alpha=1.0$ for small kd_i and gradually asymptotes to 2.0. From this plot we can determine what α was when $\delta_e=0.5d_i$. Approximating a just reconnected field line as one half a wavelength of a bent field line ($\lambda/2=2\delta_e$) yields $kd_i=\pi$. This wave number corresponds to $\alpha\approx 1.8$,

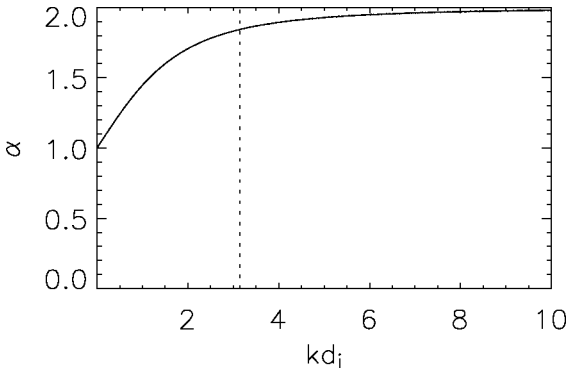

FIG. 11. The scaling exponent of the bent field line dispersion relation: α versus k, where $\omega\propto k^\alpha$.

showing that the bent field lines just outside the electron dissipation region are basically acting like whistlers when $\delta_e = 0.5$.

Both simulations clearly show the onset of a significant decrease in D when Hall physics begins to dominate the dynamics inside the dissipation region. However, the timescales for the decrease differ substantially between the two cases. In Fig. 10(a), D drops from about 20 to 5 in about 50 Ω_i^{-1}, whereas in the other case a similar drop in D takes almost ten times longer to occur. One key difference between the two cases is the relative strength of the perturbed current $\tilde{J}_z$ inside of the electron dissipation region. The electrons that are accelerated along the z direction and create this perturbed current also drag the in-plane magnetic field into the z direction and create the quadrupolar B_z synonymous with Hall mediated reconnection.[41] The perturbed current plays the dominant role in generating B_z because the equilibrium current is roughly constant along field lines ($\mathbf{B}_0 \cdot \nabla \mathbf{J}_0 \approx 0$) and does not bend the magnetic field lines to create whistler structures. Figures 10(g) and 10(h) show the average perturbed current inside the electron dissipation region, $\tilde{J}_z$, versus time. The width of the electron dissipation region, δ_e, is determined as described previously and then the average perturbed current is found inside this region. The ion current is very weak and the density change is relatively small so that $V_{ez} \approx \tilde{J}_z$. For comparison, the average equilibrium current inside the electron dissipation region (J_{z0}) is plotted as the horizontal dashed line, and the time when $\tilde{J}_z = J_{z0}$ is denoted with a square in Figs. 10(a) and 10(b). The relative location of the diamonds and squares in this figure illustrates how much stronger the electron current sheet is in the 204.8×51.2 case (run 2). When $\delta_e = 0.5$ as denoted by the vertical dotted line in Figs. 10(g) and 10(h), $\tilde{J}_z$ is ten times larger in the 204.8×51.2 case. The strength of the electron currents in the dissipation region both perpendicular to and within the plane of reconnection are clearly playing a role in determining the timescales of the transition from the developmental to the asymptotic phase. In 3D full particle simulations, faster growth of reconnection has been observed due to an acceleration of the electron current due to the lower hybrid drift instability.[45,46]

VI. ASYMPTOTIC PHASE: RECONNECTION TIMESCALES

We have demonstrated that the asymptotic inflow speed into the x-line during reconnection is approximately $0.1 c_{\mathrm{Ad}}$. A natural question to ask is whether this reconnection rate can erode magnetic flux fast enough to be consistent with the timescales of explosive energy release seen in physical systems. The case with very thin equilibrium current sheets has been shown to be fast enough (see Sec. I).[20] But, what if the equilibrium current sheet is very wide such that B_d is initially very small? We answer this question with a simple model of this asymptotic reconnection phase. Consider a reconnection dissipation region of width d_i embedded inside of a very wide current sheet with width L_0. We wish to calculate how long it will take to reconnect a given amount of magnetic flux spanning an inflow length $\xi_0 \gg d_i$. The magnetic field at the upstream edge of the dissipation region is B_{d0} initially, and the magnetic field at a distance of ξ_0 upstream of the x-line is B_0. We assume that magnetic reconnection proceeds robustly without saturation, which is valid as long as field line bending does not cause the magnetic island to saturate.[10] For simplicity, we also assume that the upstream magnetic field is uniformly convected inwards toward the x-line, which is valid as long as the tearing stability parameter Δ' [Eq. (8)] is large enough.[47] ξ is defined as the displacement of inflowing plasma and magnetic field from its initial location, and $d\xi/dt = v_{\mathrm{in}} = \alpha\, V_{\mathrm{out}}$, where $\alpha \approx 0.1$. Integrating yields the time to reconnect the length ξ_0 of magnetic flux, τ:

$$\tau = \int_0^{\xi_0} \frac{d\xi}{\alpha\ V_{\mathrm{out}}}. \tag{11}$$

We assume that a Sweet–Parker-like scaling is valid and take $V_{\mathrm{out}} = c_{Ad} = B_d / \sqrt{4\pi m_i n}$, where B_d is a function of time. At first glance, the time to reconnect a distance ξ_0 would be extremely slow, owing to the fact that $B_{d0} \ll B_0$. However, the reconnection rate grows exponentially, yielding a τ that is quite small compared to the Alfvén time based on B_{d0}, i.e. $\tau \ll \xi_0/(\alpha c_{Ad0})$. To derive this result, we calculate B_d as a function of ξ, assuming that the slope of B_d is constant upstream of the dissipation region: $B_d = B_{d0} + \xi(B_0 - B_{d0})/\xi_0$. For simplicity, we assume that the effects of changing n are small compared to the very large increase in B. Equation (11) yields

$$\tau \approx \frac{\xi_0}{\alpha c_{A0}} \ln \frac{B_0}{B_{d0}}, \tag{12}$$

where $c_{A0} = B_0 / \sqrt{4\pi m_i n}$ and we have taken $B_{d0} \ll B_0$. τ depends on the initial small upstream field B_{d0} only logarithmically. The logarithmic factor is present because the instantaneous rate of reconnection grows exponentially, and this exponential growth makes τ roughly comparable to the Alfvén time in the system based on B_0, even though $B_d \ll B_0$. If the increase of B_d with y is not linear, but some higher power, the reconnection rate will have faster than exponential growth.

Examining the case of reconnection in the solar corona is revealing because of the extremely disparate values of B_{d0} and B_0. Taking $\alpha = 0.1$, $B = 100$ G, and $n = 10^{10}$ cm^{-3}, gives $d_i \approx 200$ cm. A typical flare flux loop has a length scale of around 10^9 cm. For $\xi_0 = 10^9$ cm, $\xi_0/d_i \approx B_0/B_{d0} \approx 5 \cdot 10^6$ and thus $\tau \approx 800$ s, which is approaching the duration of an impulsive solar flare event.[7] Even though $B_{d0}/B_0 \approx 10^{-7}$, the reconnection of the whole coronal loop only takes 15 times longer than it would if $B_{d0} = B_0$.

VII. DISCUSSION AND CONCLUSIONS

In this paper, we have explored the scaling of reconnection with Hall MHD simulations in systems with embedded reconnection, i.e., a thin ion dissipation region embedded inside of a much larger equilibrium current sheet. Using the location where the ion and electron inflows decouple as the edge of the ion dissipation region, we describe a procedure

for determining the width and length of this ion dissipation region, δ and D. We determine B_d, the magnetic field at the upstream edge of the dissipation region, and V_{out}, the ion flow out of the dissipation region. After renormalizing the reconnection rate using B_d, we find that for large enough system sizes, the system asymptotes to a constant value of δ/D on the order of 0.1, which corresponds to an inflow velocity of $0.1c_{Ad}$. This value is independent of system size for cases in which a large fraction of the reconnection occurs for an island half width w that exceeds $5d_i$ with $d_i = c/\omega_{pi}$. This typically requires $L_y \geqslant 20d_i$. During this constant δ/D phase, which we call "asymptotic reconnection," a majority of island width growth occurs and a large fraction of the magnetic flux is reconnected in a very short period of time. The developmental phase of reconnection, on the other hand, is quite long and the timescales involved depend strongly on many factors, including d_i/L. A simple model for reconnection in the asymptotic phase is developed that yields timescales for explosive energy release roughly comparable to those seen in impulsive solar flares.

The asymptotic reconnection rate being independent of the system size L/d_i is seemingly at odds with several previous scaling studies.[9,11,26–28] However, the apparent differences may possibly be rectified by noting two factors: one, all of these studies include the developmental phase in their scaling of the reconnection rate, i.e., they examined the reconnection rate at times when the island width w was $\lesssim d_i$. Two, all of the studies did not renormalize the reconnection rate using a B_d determined explicitly from the simulations.

Including the developmental phase in a scaling study of the reconnection rate guarantees that the scaling of the reconnection rate will have a dependence on the microscales in the system, i.e., d_i/L, d_e/L, or ρ_s/L, where $\rho_s = c_s/(eB_{z0}/m_i c)$, and c_s is the sound speed. In forced reconnection simulations a tearing mode stable system is perturbed by deforming the boundary walls and the scaling of the maximum reconnection rate is measured.[9,26,27] However, in these simulations the total inward wall displacement was $\leqslant d_i$, meaning that at the time of the maximum reconnection rate, $w \lesssim d_i$, where w is the island half width. All of the simulations in our study that showed a clear asymptotic phase in Fig. 5(c) transitioned to the asymptotic phase when $w > 5d_i$, and therefore, $w \gg d_i$ throughout the whole asymptotic phase. If $w \lesssim d_i$, the ions are only partially magnetized in the magnetic island and the coupling of reconnection to the ion dynamics is incomplete, limiting the outflow speed to less than c_{Ad}. Indeed, during the developmental phase of reconnection in our simulations, when $w \leqslant 5d_i$, we find that V_{out} does not scale with B_d. A very interesting study would be to examine V_{out} versus B_d for a range of B_d taken at different times in a forced reconnection simulation, rather than simply examining the maximum reconnection rate as was done previously.[9,26,27]

In previous studies of the double tearing mode with a large guide field B_{z0} and a system size wide equilibrium current sheet,[11,28] the authors found that the reconnection time is given by

$$\tau_{\text{growth}} \sim \left(\frac{L_x}{\rho_s}\right)^{2/3} \left(\frac{L_x}{c/\omega_{pe}}\right) \frac{L_x}{c_{A0}}, \tag{13}$$

where $\rho_s = c_s/(eB_{z0}/m_i c)$, and c_s is the sound speed. ρ_s is the spatial scale at which dispersive kinetic Alfvén waves become active in the large guide field case and plays the same role that d_i does in the anti-parallel merging case. The results in this study, therefore, are seemingly at odds with our conclusions that the asymptotic reconnection rate is independent of d_i/L and presumably m_e/m_i. The differences between the present results and these earlier results seem to be linked to the definitions of reconnection time or rate of reconnection. Porcelli *et al.*, defined the reconnection time as the time for magnetic islands to grow from microscales ($\sim d_e$) to system size scales. Such a definition necessarily includes the developmental phase and, consistent with the present results, will be dependent on the microscales in the system. In Ref. 28, the definition of Alfvénic reconnection is given as $\tau_r \sim L_0/c_{A0}$, where L_0 is the system size and c_{A0} is the Alfvénic speed based on the asymptotic magnetic field B_0, far upstream from the dissipation region. Since the reconnection time includes the developmental phase and B_d may be significantly less than B_0, it is clear that Alfvénic reconnection with this definition is not possible.

Failing to include the changing value of B_d in the normalization of the reconnection rate makes it very difficult to discern the instantaneous scaling of δ/D. The Wang *et al.*, papers did normalize to B_d as inferred from analytical scaling arguments, but only the time of maximum reconnection rate was examined.[9,27] It is unclear, therefore, if the scaling seen persists for any significant time and follows the variation in B_d. In the other studies mentioned previously the authors did not renormalize to B_d.[11,26,28] Rewriting Eq. (7) in a more revealing form yields:

$$\left[\frac{B_0 c}{c_{A0}}\right] E_r \sim \frac{d_i}{D} B_d^2, \tag{14}$$

where we have used $\delta = d_i$. The values in the brackets are normalization values and do not change in the simulations. If the procedures for defining the ion dissipation region are used to examine other simulations, the following properties should be noted. One, Eq. (14) is only valid when $V_{\text{out}} \sim B_d$. Two, if the slope of E_r versus B_d^2 is increasing significantly then the system is probably in the developmental phase and needs to reconnect more flux before reaching the asymptotic phase.

The results of this paper are presently limited to cases with no guide field B_{z0}. A study of the scaling of that system is straightforward, however, and is planned for the future. In addition, a clear determination of when a specific system will be able to reach this asymptotic reconnection rate is necessary. This answer will depend strongly on boundary conditions, and will require careful experimental validation.

ACKNOWLEDGMENTS

This work was supported in part by NASA, NSF, and the Department of Energy. Computations were carried out at the National Energy Research Scientific Computing Center.

[1]V. M. Vasyliunas, Rev. Geophys. **13**, 303 (1975).
[2]D. Biskamp, Phys. Fluids **29**, 1520 (1986).
[3]X. Wang, Z. W. Ma, and A. Bhattacharjee, Phys. Plasmas **3**, 2129 (1996).
[4]D. A. Uzdensky, R. M. Kulsrud, and M. Yamada, Phys. Plasmas **3**, 1220 (1996).
[5]H. Ji, M. Yamada, S. Hsu, and R. Kulsrud, Phys. Rev. Lett. **80**, 3256 (1998).
[6]J. C. Dorelli and J. Birn, J. Geophys. Res. **108**, 1133 (doi:10.1029/2001JA009180, 2003).
[7]J. A. Miller, P. J. Cargill, A. G. Emslie, G. D. Holman, B. R. Dennis, T. N. LaRosa, R. M. Winglee, S. G. Benka, and S. Tsuneta, J. Geophys. Res. **102**, 14631 (1997).
[8]J. E. Borovsky, R. J. Nemzek, and R. D. Bellan, J. Geophys. Res. **98**, 3807 (1993).
[9]X. Wang, A. Bhattacharjee, and Z. W. Ma, J. Geophys. Res. **105**, 27633 (2000).
[10]R. B. White, Rev. Mod. Phys. **58**, 183 (1986).
[11]D. Grasso, F. Pegoraro, F. Porcelli, and F. Califano, Plasma Phys. Controlled Fusion **41**, 1497 (1999).
[12]B. Lembege and R. Pellat, Phys. Fluids **25**, 1995 (1982).
[13]R. Pellat, F. V. Coroniti, and P. L. Pritchett, Geophys. Res. Lett. **18**, 143 (1991).
[14]M. I. Sitnov, A. S. Sharma, P. N. Guzdar, and P. H. Yoon, J. Geophys. Res. **107**, 1256 (doi:10.1029/2001JA009148, 2002).
[15]F. Porcelli, Phys. Rev. Lett. **66**, 425 (1991).
[16]H. P. Furth, J. Killeen, and M. N. Rosenbluth, Phys. Fluids **6**, 459 (1963).
[17]M. A. Shay, J. F. Drake, B. N. Rogers, and R. E. Denton, Geophys. Res. Lett. **26**, 2163 (1999).
[18]M. A. Shay and J. F. Drake, Geophys. Res. Lett. **25**, 3759 (1998).
[19]M. Hesse, K. Schindler, J. Birn, and M. Kuznetsova, Phys. Plasmas **6**, 1781 (1999).
[20]M. A. Shay, J. F. Drake, B. N. Rogers, and R. E. Denton, J. Geophys. Res. **106**, 3751 (2001).
[21]P. L. Pritchett, J. Geophys. Res. **106**, 3783 (2001).
[22]P. Ricci, G. Lapenta, and J. U. Brackbill, Geophys. Res. Lett. **29**, 2088 (doi:10.1029/2002GL015314, 2002).
[23]J. Birn, J. F. Drake, M. A. Shay, B. N. Rogers, R. E. Denton, M. Hesse, M. Kuznetsova, Z. W. Ma, A. Bhattacharjee, A. Otto *et al.*, J. Geophys. Res. **106**, 3715 (2001).
[24]M. M. Kuznetsova, M. Hesse, and D. Winske, J. Geophys. Res. **106**, 3799 (2001).
[25]B. N. Rogers, R. E. Denton, J. F. Drake, and M. A. Shay, Phys. Rev. Lett. **87**, 195004 (2001).
[26]R. Fitzpatrick, Phys. Plasmas **11**, 937 (2004).
[27]X. Wang, A. Bhattacharjee, and Z. W. Ma, Phys. Rev. Lett. **87**, 265003 (2001).
[28]F. Porcelli, D. Borgogno, F. Califano, D. Grasso, M. Ottaviani, and F. Pegoraro, Plasma Phys. Controlled Fusion **44**, B389 (2002).
[29]D. Biskamp, E. Schwarz, and J. F. Drake, Phys. Rev. Lett. **75**, 3850 (1995).
[30]M. A. Shay, J. F. Drake, R. E. Denton, and D. Biskamp, J. Geophys. Res. **25**, 9165 (1998).
[31]M. Hesse, M. Kuznetsova, and J. Birn, J. Geophys. Res. **106**, 29831 (2001).
[32]P. Rutherford, Phys. Fluids **16**, 1903 (1973).
[33]B. D. Jemella, M. A. Shay, J. F. Drake, and B. N. Rogers, Phys. Rev. Lett. **91**, 125002 (2003).
[34]P. A. Sweet, in *Electromagnetic Phenomena in Cosmical Physics*, edited by B. Lehnert (Cambridge University Press, New York, 1958), p. 123.
[35]E. N. Parker, J. Geophys. Res. **62**, 509 (1957).
[36]V. A. Sergeev, D. G. Mitchell, C. T. Russel, and D. J. Williams, J. Geophys. Res. **98**, 17345 (1993).
[37]M. Hoshino, A. Nishida, T. Mukai, Y. Saito, and T. Yamamoto, J. Geophys. Res. **101**, 24775 (1996).
[38]Y. Asano, T. Mukai, M. Hoshino, Y. Saito, H. Hayakawa, and T. Nagai, J. Geophys. Res. **108**, 1189 (doi:10.1029/2002JA009785, 2003).
[39]A. Runov, R. Nakamura, W. Baumjohann, R. A. Treumann, T. L. Zhang, M. Volwerk, Z. Vörös, A. Balogh, K.-H. Glabmeier, B. Klecker *et al.*, Geophys. Res. Lett. **30**, 1579 (doi: 10.1029/2002GL016730, 2003).
[40]D. A. Uzdensky and R. M. Kulsrud, Phys. Plasmas **7**, 4018 (2000).
[41]M. E. Mandt, R. E. Denton, and J. F. Drake, Geophys. Res. Lett. **21**, 73 (1994).
[42]M. Ottaviani and F. Porcelli, Phys. Rev. Lett. **71**, 3802 (1993).
[43]R. Horiuchi and T. Sato, Phys. Plasmas **1**, 3587 (1994).
[44]Z. W. Ma and A. Bhattacharjee, Geophys. Res. Lett. **23**, 1673 (1996).
[45]M. Scholer, I. Sidorenko, C. H. Jaroschek, and R. A. Treumann, Phys. Plasmas **10**, 3521 (2003).
[46]I. Shinohara and M. Fujimoto, ''Quick triggering of magnetic reconnection in an ion-scale current sheet,'' Phys. Rev. Lett. (submitted).
[47]D. Biskamp, *Magnetic Reconnection in Plasmas* (Cambridge University Press, Cambridge, UK, 2000).